Journal of Structural Geology, Vol. 5, No. 3/4, pp. 455 to 463, 1983
Printed in Great Britain

0191-8141/83 $3.00 + 0.00

Strain patterns in an ice cap and implications for strain variations in shear zones

PETER J. HUDLESTON

Department of Geology and Geophysics, University of Minnesota, Minneapolis, MN 55455, U.S.A.

(*Received* 7 *September* 1982; *accepted in revised form* 2 *December* 1982)

Abstract—Glacier flow is a form of gravity tectonics in thin sheets, characterized by the development of large strains, foliation and folds. Strain is difficult to measure in ice, but numerical methods provide a good means of estimating cumulative strains. In simple terms, flow in an ice cap involves vertical flattening at the center with bottom-parallel shear increasing in intensity downwards and outwards. In steady state, cumulative strains will be plane if flow is two-dimensional, as in parts of many valley glaciers and some ice caps, and of flattening type if lateral extension occurs normal to the flow direction, as in many ice sheets. In both radial and plane flow, strain gradients will be large vertically and low horizontally outwards. Cumulative strain magnitude can be extremely large near the base and at the margin. Z is everywhere sub-vertical.

If flow is unsteady, more complex strain patterns develop, even if changes in the flow field are slight. Over bedrock ridges, flow perturbations can lead locally to rotations greater than those of the quasi-simple shear acting near the base in steady state flow. This may cause the X-direction of the cumulative strain to rotate through the 'shear plane' in the neighborhood of the perturbation, in which case strain magnitudes subsequently diminish, leading to low or zero strains in plane flow, and to constrictional strains in radial flow. In the latter case, X lies horizontal and perpendicular to the flow direction, and we have local constrictional strain in an overall flattening field. The zones of perturbed strain tend to be associated with the inverted limbs of recumbent folds.

Shear zones in rocks are expected to show similar patterns of strain perturbation.

INTRODUCTION

THE ANALOGY between flow in glaciers or ice sheets and tectonic flow in rocks has often been made (e.g. Wegmann 1963, Ragan 1969, Hambrey 1977). Glacier flow is a kind of thin-skinned tectonics, driven by gravity, which may have its equivalent in rocks in certain kinds of nappe structure. Because the basal and lateral parts of ice caps and glaciers constitute shear zones, strain patterns and structural development there and in shear zones in rocks should be similar. Deformation in ice is by both brittle and ductile processes. Brittle behaviour by crevassing is common near the upper surface of a glacier, where flow is extensional. Flow is ductile elsewhere and involves basal glide, grain rotation and recrystallization. Very large strains may develop and characteristic structures appear, the most prominent of which are foliation and folds (Allen *et al.* 1960, Hambrey 1975, Hudleston 1976a, 1977a, Hambrey & Müller 1978, Hooke & Hudleston 1978). Rather similar structures, developed under similar kinematic conditions, are also found in salt glaciers (Talbot 1979).

Knowledge of the nature of the strain that develops is important for understanding structures and, conversely, structures may provide useful information on strain. Good strain markers are hard to come by in ice, but bubble shape and orientation can be used in weakly deformed ice (Hudleston 1977b) and there is also the potential for using bubble distribution with methods such as those developed by Fry (1979). Perhaps the best approach for estimating strain in glaciers is by making use of measured or calculated velocity distributions (Milnes & Hambrey 1976, Hambrey & Milnes 1977, Hooke & Hudleston 1980), from which particle paths and cumulative strains may be computed numerically. Although the precise history of flow is never known for any glacier, geomorphological observations often provide information on past configurations (e.g. Hudleston & Hooke 1980) which in turn provide control on past flow fields. Even with quite large changes in external configuration, due to glacier advance or retreat, the basic internal pattern of velocity and stain rate will not change greatly. However, small local changes in the internal velocity field caused by modest changes in external glacier configuration may eventually lead to large local variations in cumulative strain. It is the purpose of this paper to study such variations by extending earlier work to include the cases in which (i) flow is non-planar and (ii) perturbations from the steady state occur. The strain variations and structures that result are also likely to be found in shear zones in rocks, in which unsteadiness of flow has occurred.

NUMERICAL MODEL FOR STEADY-STATE PLANE FLOW

The simplest case to deal with is that in which flow is two-dimensional and steady. There are a number of instances of glacial flow approximating this state (e.g. Budd 1969, Hudleston 1976a). The principle of the method by which particle paths and cumulative strains are found is given in detail in an earlier publication (Hudleston & Hooke 1980) and will not be repeated here. The results from this earlier work, with application to part of the Barnes Ice Cap in Baffin Island, Canada,

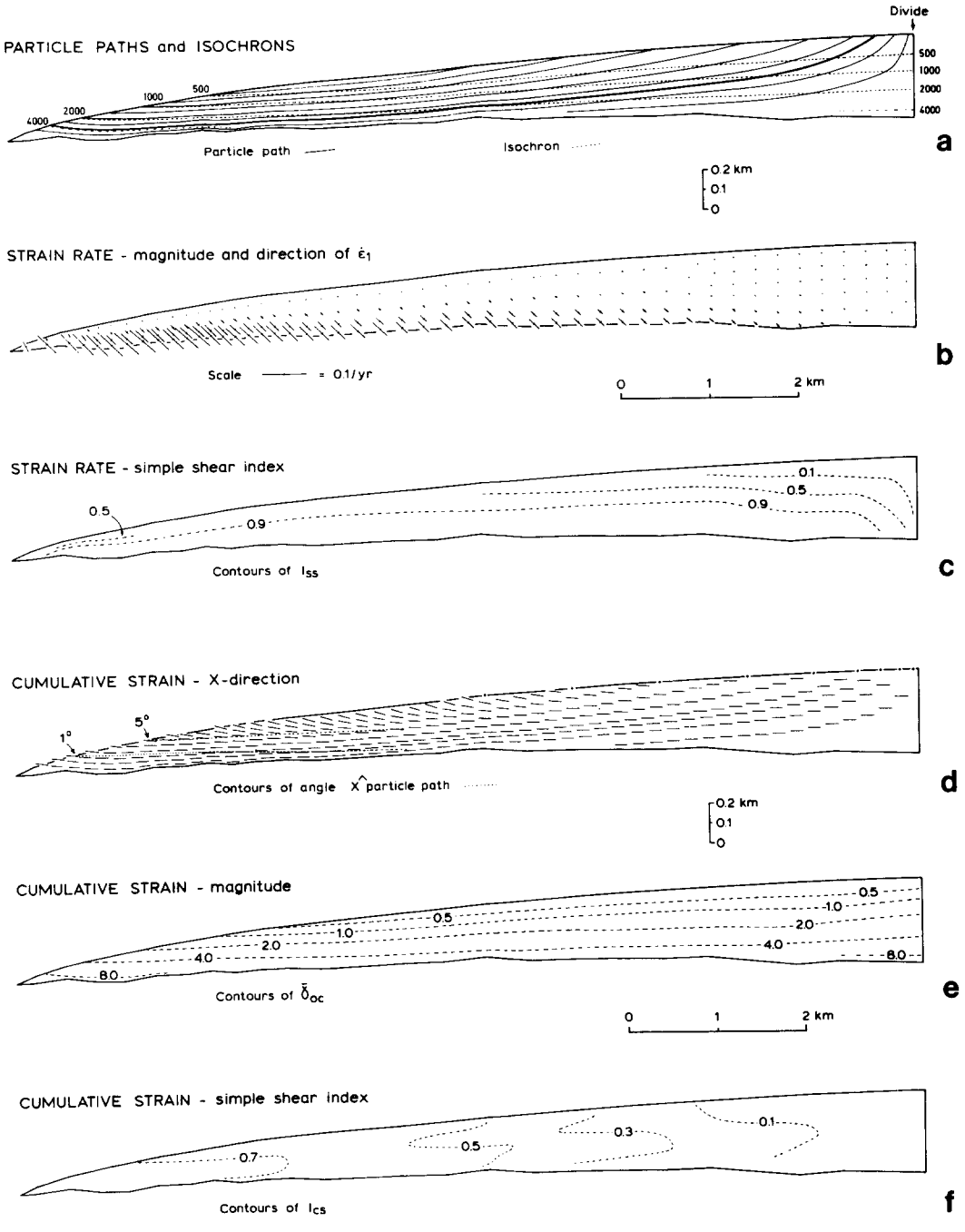

Fig. 1. Steady state flow and deformation in a section of the Barnes Ice Cap (after Hudleston & Hooke 1980). (a) Particle paths and isochrons, with contours in years. (b) Magnitudes and true orientations (no vertical exaggeration) of maximum principal strain rate $\dot{\epsilon}_1$. (c) Contours of simple shear index. (d) Bars showing true orientation of the X-direction of cumulative (finite) strain. (e) Contours of cumulative strain magnitude. (f) Contours of simple shear index.

are summarized here in order to provide continuity and comparison. Here, steady state means the velocity field and glacier configuration remain unchanged with time. Long-term steady state can sometimes be assumed, and the problem of finding a satisfactory steady state velocity field has been discussed earlier for a section of the Barnes Ice Cap (Hudleston & Hooke 1980). In that case, horizontal velocities were derived from surface measurements, borehole data, use of the flow law, and knowledge of the fact that the ice is frozen to the bedrock. Vertical velocities were then found from mass balance considerations.

For the purpose of computation, the velocity field, once selected (see Hudleston & Hooke 1980), is represented by its values at the nodes of a triangular grid of elements. The velocity at any point can then be found by linear interpolation and, by using short increments of displacement, individual particles of ice can be followed through the glacier to approximate smooth particle paths and flow lines (Fig. 1a). Strain rate is constant within each triangular element. Incremental strains can readily be found from the deformation matrix associated with each increment of displacement, and cumulative strains found by multiplying together the incremental deforma-

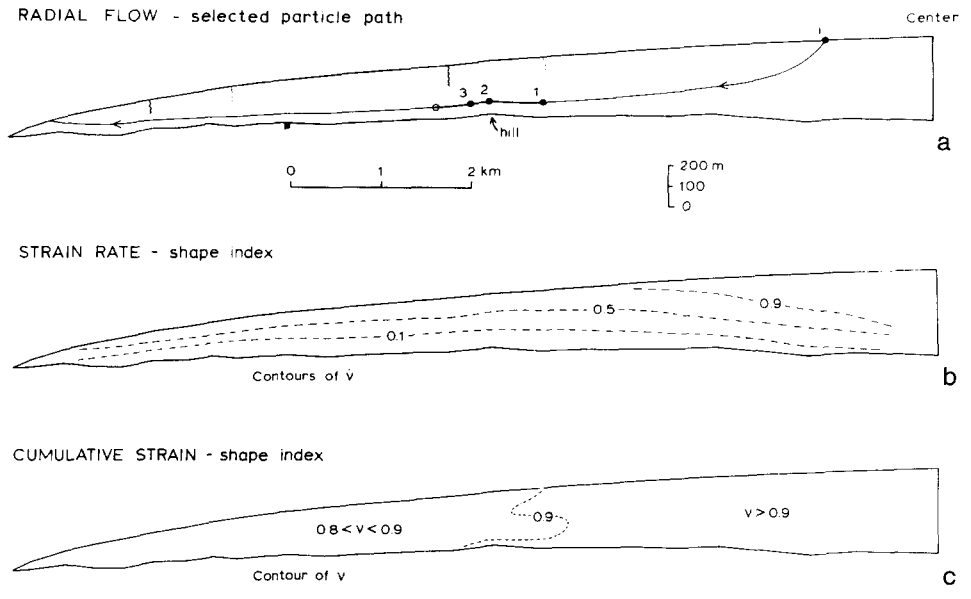

Fig. 2. Same section as in Fig. 1, with steady-state flow, modified to become radial. (a) Selected particle path and numbered particles used in tracing perturbation. Vertical wavy lines show limits of Fig. 6 (light) and Fig. 7 (heavy). (b) Contours of shape index for strain rate ($\dot{\nu}$), (see text). (c) Contour of shape index for cumulative strain (ν), (see text).

tion matrices (Hudleston & Hooke 1980). The axes of the cumulative strain ellipsoid are denoted by X, Y and Z (with $X \geqslant Y \geqslant Z$).

Results

The results for the Barnes Ice Cap are shown in Fig. 1. The pattern of flow and strain rate is clear; it is almost that expected for simple shear near the base of the glacier and pure shear at the surface and along the center line (Fig. 1c). The index of simple shear is defined by $I_{ss} = 2\dot{\omega}/(\dot{\epsilon}_1 - \dot{\epsilon}_3)$, where $\dot{\omega}$ is the rotational component of the deformation rate tensor and $\dot{\epsilon}_1$ and $\dot{\epsilon}_3$ are maximum and minimum principal strain rates (Hudleston & Hooke 1980). I_{ss} has a value of 1.0 for simple shear and 0.0 for pure shear. Cumulative strain is characterized by X being subhorizontal near the base and center, and plunging gently up-glacier elsewhere. In much of the ice, X makes a very small angle with the particle paths and also with the isochrons, which are manifest as primary stratification (Figs. 1a & d). Strain gradients are very high vertically and low horizontally (Fig. 1e): very large strains are encountered at the base. Strain magnitude is measured by $\bar{\gamma}_o$, the natural octahedral unit shear, defined by:

$$\bar{\gamma}_o = 2/3[(\bar{\epsilon}_1 - \bar{\epsilon}_2)^2 + (\bar{\epsilon}_2 - \bar{\epsilon}_3)^2 + (\bar{\epsilon}_3 - \bar{\epsilon}_1)^2]^{1/2}$$

where $\bar{\epsilon}_1 = \ln(1 + e_1)$, etc. and $(1 + e_1)$ is a principal semi-axis of the strain ellipsoid. The index of simple shear, I_{cs}, is found by dividing the actual rotational component of the deformation by the rotation that would result from a simple shear of magnitude $\bar{\gamma}_o$. I_{cs} also has a value of 1.0 for simple shear and 0.0 for pure shear (Fig. 1f).

MODIFICATION FOR RADIAL FLOW

Many ice caps, such as the Barnes, are roughly circular in overall plan and therefore involve divergent flow, such that there is horizontal extension perpendicular to the flow lines as seen in map view. To demonstrate the effect of such flow on the strain pattern it is convenient to take the case of perfect radial flow. This is done in the following artificial way, using the same glacier configuration as for plane flow (Fig. 1). The longitudinal strain rate, $\dot{\epsilon}_{zi}$, perpendicular to the 'flow plane', xy (the plane of Fig. 1 with x in the direction of flow measured from the center and y vertical), at any point i is given by $\dot{\epsilon}_{zi} = u_i/x_i$, where u is the horizontal component of velocity. The x-component of strain rate, $\dot{\epsilon}_{xi}$, is derived directly from the original horizontal velocities and $\dot{\epsilon}_{yi}$ is found from constancy of volume ($\dot{\epsilon}_x + \dot{\epsilon}_y + \dot{\epsilon}_z = 0$). Vertical velocities are found by integration of $\dot{\epsilon}_{yi}$ from the base up.

Results

The pattern of flow lines and particle paths looks very similar to that for plane flow: one selected particle path is shown in Fig. 2(a). The magnitudes and orientations of principal strain rates and cumulative strains in the plane of flow are also very similar to those found in plane flow and are not shown. A significant difference occurs, however, in the symmetry or shape of the strain. Strains and strain rates are all of the flattening type, but the degree of flattening varies with position in the glacier. To illustrate this Lode's number, ν, is used

$$\nu = \frac{2\bar{\epsilon}_2 - \bar{\epsilon}_1 - \bar{\epsilon}_3}{\bar{\epsilon}_1 - \bar{\epsilon}_3}.$$

This has a value of +1.0 for pure flattening (oblate

ellipsoid), −1.0 for pure constriction (prolate ellipsoid), and 0.0 for plane strain. A similar quantity, $\dot{\nu}$, can be defined for strain rate, replacing $\bar{\epsilon}_1$ by $\dot{\epsilon}_1$, etc.

Reference to Fig. 2 shows that strain rate is closest to plane strain (and simple shear) near the base of the glacier where $\dot{\epsilon}_x$ and $\dot{\epsilon}_y$ are large in relation to $\dot{\epsilon}_z$. Cumulative strain is strongly of flattening type throughout the glacier, but does become less oblate away from the center. It should be noted that plots of shape index for plane flow would show no contours—the indices ν and $\dot{\nu}$ have values of zero everywhere.

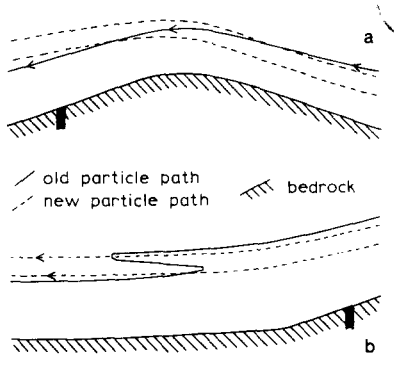

Fig. 3. (a) Schematic steady-state particle paths over bedrock hill, just before and just after 'instantaneous' perturbation. (b) Old particle path transformed into fold by flow on new particle path.

PERTURBATION OF FLOW—GENERAL CONSIDERATIONS

Steady-state flow for any length of time in a glacier is unlikely, and most glaciers have undergone significant fluctuations since the end of the Pleistocene. Under steady-state flow, sedimentary layering and foliation form a simple pattern, and passive folding of these cannot occur (excluding broad scale, open folding associated with nonlinear displacement gradients towards the sides and base of glaciers and with the curvature of particle paths, Hudleston 1976a, Hudleston & Hooke 1980) . Perturbations of flow associated with changes in glacier configuration are required to allow small-scale passive folds to form, and such folds appear to be common in virtually all glaciers. The perturbations that give rise to folds must also disturb the strain field, and this is the main concern here.

In order to examine the principles of strain perturbation, it is most convenient to use the analogy of simple shear, which is good for the basal parts of the glacier. The shear planes will be sub-parallel to the bedrock surface. A change with time in ice thickness or surface slope, associated with advance or retreat of the glacier, changes the boundary conditions for the flow, which in turn causes a slight change of the velocity field within the ice. If the changed conditions remain fixed, a new steady state exists, with a new set of particle paths and flow lines oblique to the old (Fig. 3a). Over hills or valleys in the bedrock, the change in flow regime may cause the old particle paths to be transformed into subsimilar recumbent folds (Fig. 3, Hudleston 1977a). If sedimentary layering or foliation is parallel or nearly parallel to the old particle paths, the folds will have a physical manifestation. The sense of asymmetry is dictated by the sense of shear and the fact that the layering before perturbation is subparallel with the shear planes (see also Cobbold & Quinquis 1980).

In an earlier study (Hudleston 1976b), the strain that accumulated *after* the perturbation was examined. In a small area affected by folding, this strain was quasi-homogeneous, with XY parallel to the axial surfaces of the folds. This reflects the fact that the strain developed under a new steady state forms the same simple pattern as that developed under an old. The pattern of total strain, which has not been considered previously, is not so simple.

Under steady flow near the base of a glacier, the cumulative strain ellipse progressively becomes more elliptical and makes smaller angles with the shear plane. In simple shear, each value of shear strain, γ, is associated with a strain ellipse of unique ratio and orientation (e.g. Ramsay 1980, fig. 8). After a perturbation of the kind sketched in Fig. 3, the strain ellipse will make a different angle with the new shear plane. This angle may be greater or less than the original, or even negative. A negative angle means, in effect, that the strain ellipse has rotated through the shear plane (with 'new' and 'old' shear planes taken as a single reference plane). In all the cases which lead to passive folding (Hudleston 1976a), the angle of the strain ellipse (X) to the shear plane is reduced and may become negative.

If the angle, θ, between strain ellipse and shear plane is positive after the perturbation, the cumulative strain will continue to increase in magnitude and X make smaller angles with the shear plane, but in a way not directly given by the equations of simple shear. Further deformation can be considered as the superposition of a simple shear on a pre-existing strain of constant axial ratio, whose orientation with respect to the shear plane is given by the degree of perturbation. Standard equations for successive deformations (e.g. Elliott 1972) can be used for the calculations.

Using the analogy of ideal simple shear, the history of deformation following a perturbation can be examined in the following way. If θ is negative, deformation after perturbation can follow one of three paths. In the first case, a special one, θ is such as to make the ellipse a reciprocal strain ellipse for continued simple shear on the new shear planes. Let this angle be θ_c. Further flow will cause the ellipse to revert to a circle or isotropic point (Brun, this issue), after which the strain will increase again with positive θ (Fig. 4a). On a natural-strain plot, the strain path is from A to B and back towards, and eventually beyond, A (Fig. 4a).

If $\theta < \theta_c$, continued simple shear will cause both the magnitude of the cumulative strain and θ to decrease. A minimum magnitude is reached when $\theta = 0$; subsequently strain magnitude and orientation increase in a way that mirrors the path of the decrease. On the strain

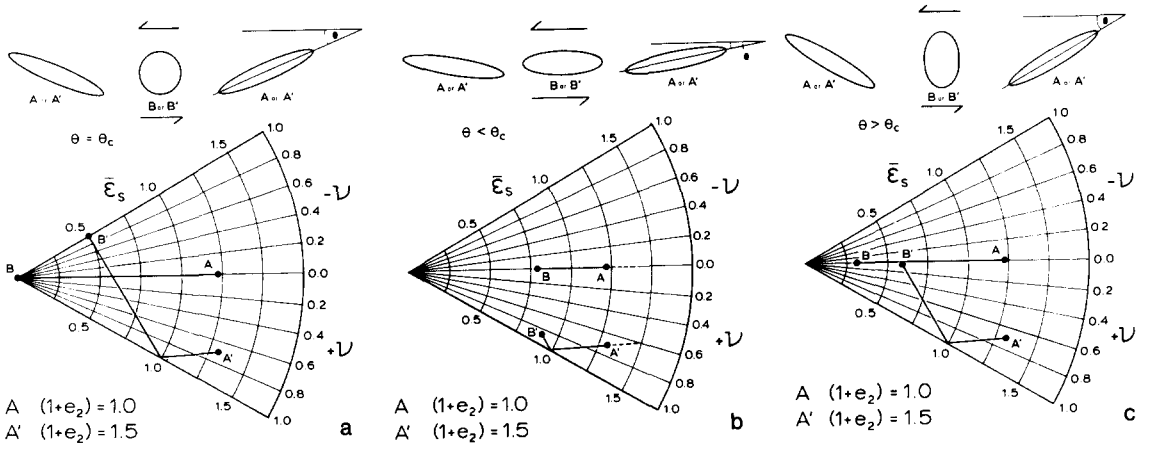

Fig. 4. Strain ellipses and strain paths subsequent to a hypothetical perturbation that leaves strain ellipse A or A′ at angle θ to the plane of simple shear. The primed letters indicate a constant extension in the third dimension. The strain coordinate, $\bar{\epsilon}_s = (\sqrt{3}/2)\gamma_0$ is a standard one for strain plots (see Hossack 1968). The three cases (a), (b) and (c) are described in the text.

plot, the path is from A to B and back to A and beyond (Fig. 4b).

If $\theta > \theta_c$, a similar sequence of changes occurs, except that θ increases after the perturbation and the minimum strain occurs when $\theta = 90°$ (Fig. 4c).

Now, if the starting state is not true simple shear, but involves a constant strain in the third dimension, the pattern of strain in the xy-plane (perpendicular to the shear plane) remains the same as for plane strain for the three cases presented. However, the symmetry and magnitudes of the three-dimensional strains are quite different. With glaciers in mind, let us take the case where $(1 + e_2) = 1.5$. The ratio $(1 + e_1)/(1 + e_3)$ remains the same as for plane strain, but the absolute values of e_1 and e_3 change to maintain constant volume. In the case where $\theta = \theta_c$, the initial state lies in the flattening field at A′ on the strain plot (Fig. 4a). After the perturbation, as the strain decreases in magnitude, the strain path passes through a state of pure flattening ($\nu = 1.0$) on the way to a state of pure constriction ($\nu = -1.0$) at B′, at the point of minimum strain (Fig. 4a). Further deformation retraces the path towards A′.

In the other two cases, similar strain paths are followed (Figs. 4b & c) but pure constriction is not reached. The degree to which this is approached, and whether or not the constrictional field is even entered, depends on the difference between θ and θ_c: the smaller the difference, the closer the approach to pure constriction.

EXAMPLE OF PERTURBATION OF GLACIAL FLOW

The kind of perturbation of cumulative strain described above is expected to occur in glaciers. The effect on the total strain field of a perturbation of plane flow has not been considered previously. Many consequences of perturbation are identical for plane flow and radial flow. The differences between the two cases will be discussed after the slightly more complex and interesting case of radial flow has been considered.

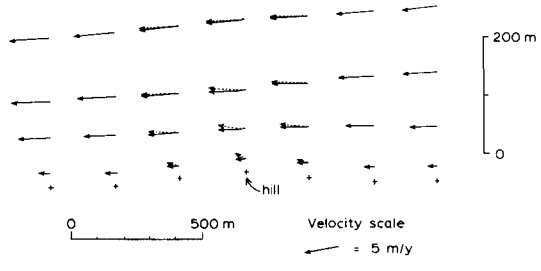

Fig. 5. Velocity vectors before (solid) and after (dashed) perturbation used in strain modelling, at nodes of a grid of elements in the vicinity of the hill shown in Fig. 2. Away from the three central columns of nodes, there is no change in velocity. The complete grid is almost the same as that illustrated in Hudleston & Hooke (1980 fig. 2B).

With a knowledge of the effects of changing ice thickness or surface slope gained from earlier work (Hudleston 1976a), the following simple procedure was used to apply a local arbitrary perturbation to the pattern of radial flow described above. This simulates the effect of ice advance or retreat, without having to change the configuration of the glacier and the whole velocity field, and so simplifies the computations.

An 'instantaneous' modification of the vertical velocity was made at a few selected nodes above the hill indicated in Fig. 2. This hill, present on the particular cross-section of the Barnes Ice Cap under study, was chosen as a matter of convenience for demonstrating the principle: restriction to a single hill and perturbation emphasizes the nature of the phenomenon. Upward perturbations were added to the velocities at nodes immediately above the hill crest, and lesser perturbations were added at the nodes in columns either side. The perturbations were made to die out exponentially upwards in each column of nodes (Fig. 5). The velocities in all other nodes were left unchanged. This type of perturbation simulates the effects of a glacial retreat (see Hudleston 1976a, fig. 7a). Once applied, the perturbed velocities are held fixed, thus making an instantaneous change from an old to a new steady state. The magnitudes and nature of the perturbed velocities were

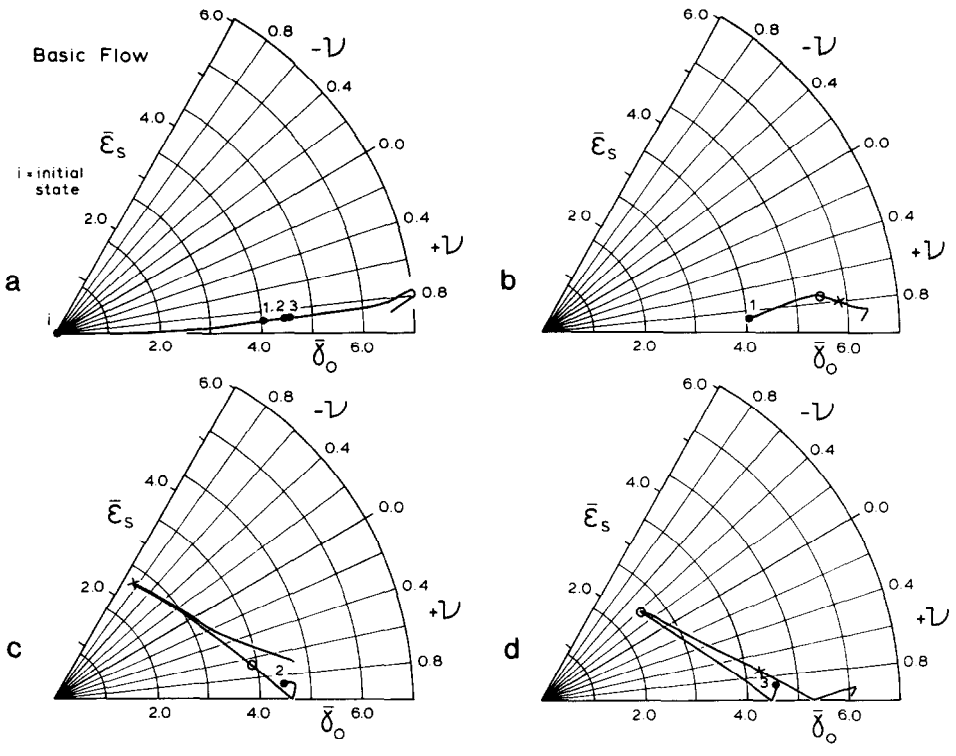

Fig. 6. Strain paths for radial flow: (a) for points lying on the particle path of Fig. 2(a) or for particles following this path in steady state and (b)–(d) for particles 1, 2 and 3 after perturbation. Circles and crosses correspond to positions of particles 345 and 530 years, respectively, after perturbation.

varied, and the effects on the subsequent deformation pattern studied. One particular model was chosen that illustrates nicely the case in which the pre-existing strain ellipses are rotated through the new shear plane, and consequent large modifications to the cumulative strain result.

With the velocity field known, before and after perturbation, the computation of displacement and strain comes from the application of the method referred to above and described in detail in Hudleston & Hooke (1980). The only new feature is the addition of a strain in the third dimension, found for each increment by multiplying strain rate by the increment of time. Before the perturbation is applied, we have the pattern of flow and strain as shown in Fig. 2. Points 1, 2 and 3 all lie on the same particle path (Fig. 2a). The states of strain at these points are represented by dots in Fig. 6(a). The heavy line passing through these dots is the strain path, followed by all particles of ice on this particular path (in the absence of perturbations). The end of the strain path (Fig. 6a) corresponds to the point where ablation occurs (Fig. 2a).

When the velocities over the hill (below points 1, 2 and 3) are perturbed, each particle is displaced onto a new path, different for each particle. The new particle paths, not shown in Fig. 2, would not individually appear very different from the one shown. The situation at two selected stages after the perturbation is shown in Figs. 7 and 8. The old path containing particles 1, 2 and 3 has become deformed into a recumbent fold, which would be visible as such if a layering or foliation were parallel or nearly parallel to the old particle paths (e.g. Hudleston 1976a, fig. 2). The transformed positions of old particle paths above and below the main one (Figs. 7 and 8) show how the fold dies out upwards and grows downwards toward the hill above which the fold was seeded. Not shown is the eventual dying out of the fold near the hill.

The strain history for a particle initially downstream from the hill is no different from that for the unperturbed flow (since such particles underwent no perturbation). The strain history for particles initially upstream from the hill is only modestly affected by the perturbation. For example, particle 1 (Figs. 2, 7 and 8) is carried over the hill on a new path higher than the old, but it follows a strain path (Fig. 6b) not greatly different from its unperturbed equivalent (Fig. 6a). The situation for particles 2 and 3, which lay directly above the hill at the time of perturbation, is quite different. The strain history for particle 2 is similar to that shown in Fig. 4(c), passing through a state of pure flattening to almost pure constriction (Fig. 8) and back again to the flattening field before ablation. Particle 3 undergoes a similar history, but is 'out of phase' with particle 2: it reaches its minimum strain in the constrictional field earlier (Fig. 7), at a time when particle 2 is still well within the flattening field ($\nu = 0.7$). Also, particle 3 returns to a state of pure flattening once again before ablation.

The strain paths of the glacial model (Fig. 6) differ from those of the ideal model (Fig. 4) in two respects, both due to the flow in the glacier departing from simple shear. First, after the excursion into the constrictional

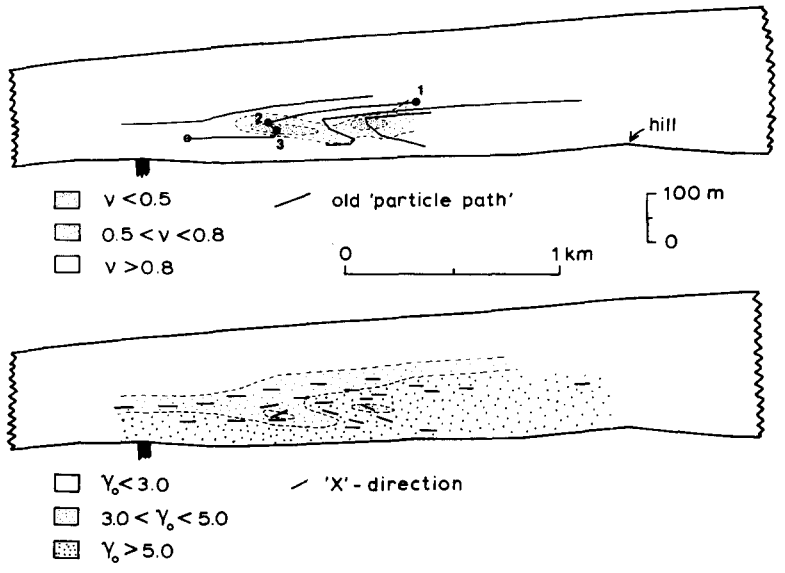

Fig. 7. Symmetry, magnitude, and true orientation of cumulative strain, 345 years after perturbation.

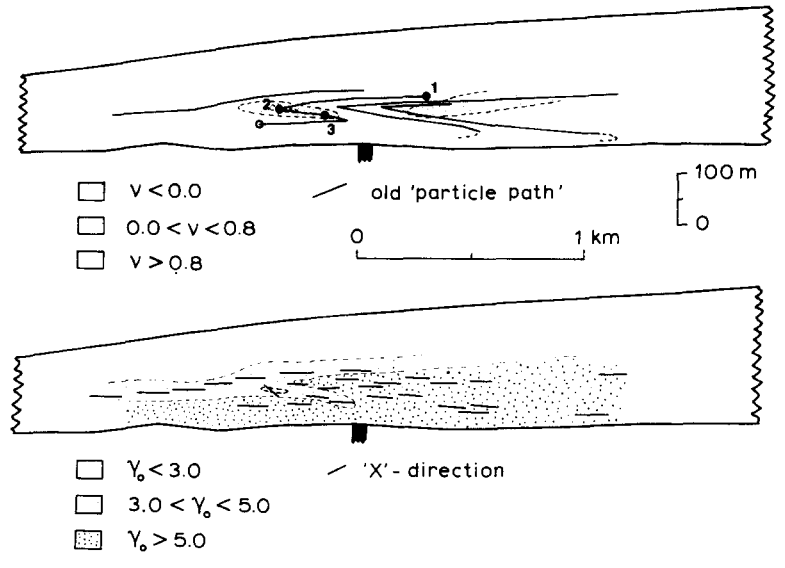

Fig. 8. As Fig. 6, 530 years after perturbation. The black object embedded in the bedrock helps show the relative position of this section with respect to the sections of Figs. 2 and 7.

field, the return to flattening in the glacial model is not exactly by the same path. This largely results from the strain in the third dimension, which is unaffected by the perturbation and increases monotonically with outward flow: the strain magnitudes on returning to the flattening field are therefore greater than those on departure from it. Second, the hook found at the end of the strain paths of the glacial model is not present in those of the ideal models. This is due to the longitudinal compressive strain existing in the distal parts of the glacier, causing strain magnitude to be diminished and the hook to appear.

It is apparent that the cumulative strain of any particle of ice has a relatively brief excursion away from the flattening field, and that after this excursion it returns to a path not very different from the one it was originally following. The *pattern* of strain perturbation, however, exists for much longer than the time spent by any individual particle of ice on its excursion, since the excursion of each is offset in time from that of its neighbours: different particles reach positions of maximum excursion and minimum strain at different times.

The detailed pattern of strain perturbation depends on the nature of the velocity perturbation and cannot be accurately or realistically determined from the rather crude modelling done here. It does seem, however, that the perturbed zone, of low strain magnitude and departure from flattening symmetry, will have a more or less lensoid form (Figs. 7 and 8). Principal strain orientations in the perturbed zone will often be at high angles to the horizontal, due to the ellipse rotating in the manner

illustrated in Fig. 4; strain trajectories may in fact trace out folded forms much like the old particle paths.

If, instead of radial flow, the simpler case of plane flow were taken, the appearance of the perturbed strain field in cross-section would be almost identical to that shown in Figs. 7 and 8. Strain magnitudes would show a similar reduction in the overturned limb of the 'folded particle paths', but strain symmetry, as described and illustrated above for idealized simple shear (Fig. 4), would not, of course, vary. It would be everywhere given by $\nu = 0.0$.

DISCUSSION AND CONCLUSIONS

The most interesting result of this study is that it is possible, by perturbing flow which is basically simple shear, to produce local zones of low strain in regions of overall high strain. Moreover, if an element of extension in the third dimension is added, it is possible to produce zones of constrictional strain in an otherwise flattening field. In this case the axis of constriction, X, lies parallel to the shear plane and perpendicular to the shear direction.

These types of strain perturbation predicted for glaciers are probably important for rocks too, in particular in shear zones, where there are various ways of introducing perturbations into the flow (Cobbold & Quinquis 1980). The juxtaposition of zones of flattening and constrictional strain in rocks has been noted by several authors (e.g. Hossack 1968, Clifford 1972, Hudleston 1976b), and some of these juxtapositions may result from the kind of process described here. It should be noted, though, that the X-direction of strain in zones (themselves rod-shaped) of local constriction described by Hossack lies in the presumed direction of movement in a thrust zone, not perpendicular to it as would be expected by the process described here. Another way of producing strain variations in shear zones or thrust belts has been suggested by Coward & Potts (this issue), who consider deformation near the terminations or edges of propagating shear zones or thrusts. Local flattening or constrictional strains can be predicted in these locations. Other examples of juxtaposition of constrictional and flattening fabrics, produced by superimposed deformation, have been described by Goldstein (1980) and Duncan (1982).

The relationship of the zone of anomalous strain to folding is of interest. The folds produced in pre-existing layering or foliation (parallel or sub-parallel to the old particle paths) are closely related in origin and in space to the perturbations of total strain. We see that the lensoid zone of low strain lies in or adjacent to the hinges and *overturned* limb of such a fold (Figs. 7 and 8). This predicted relationship should provide a useful means of identifying this phenomenon in rocks. Many recumbent folds, such as the Morcles nappe (Ramsay 1981, fig. 5), clearly develop by localized shear within the inverted limb. They, thus, represent quite a different phenomenon, in which the existence of the folds is largely due to the localization of strain, and strain magnitudes are greatest in the inverted limb. In the process described in this paper, the strain developed *after* the perturbation of flow is fairly homogeneous across the folds (Hudleston 1977a), and no localization of this strain occurs. It is not clear if the folds developed in salt glaciers are associated with similar patterns of strain. It is unlikely, perhaps, since the incremental strains, as indicated by halite porphyroclasts, appear to vary across the fold (Talbot 1979, fig. 6), rather than stay more or less constant.

Further complications may arise if, as seems likely, the disturbance that causes the strain perturbation and folds is not two-dimensional, as assumed everywhere above, but is more complex. A conical hill at the base of the glacier would produce a point disturbance and a sheath fold would result from the subsequent flow. I have seen examples of such folds in glaciers and they are common in shear zones in rocks (e.g. Minnigh 1979, Cobbold & Quinquis 1980). The pattern of cumulative strain following such a perturbation would be quite complicated, even if the overall strain field is one of simple shear alone. The zone of strain disturbance will be limited in the third dimension, and may be cigar shaped itself.

Folds resulting from perturbed flow are very common in glaciers and also common in rocks such as mylonites in which large shear strains have developed. If the folds develop in a passive manner, strain markers that record the whole deformation should indicate the kind of strain variations described in this paper. Such strain variations may well prove to be common.

Acknowledgements—This research was supported financially by the U.S. National Science Foundation (Grant EAR-7712990). The manuscript has benefited from the comments and constructive criticisms of an anonymous reviewer.

REFERENCES

Allen, C. R., Kamb, W. B., Meier, M. F. & Sharp, R. P. 1960. Structure of the lower Blue Glacier, Washington. *J. Geol.* **68**, 601–625.

Brun, J. P. 1983. Isotropic points and lines in strain fields. *J. Struct. Geol.* **5**, 321–327.

Budd, W. F. 1969. The dynamics of ice masses. *Australian National Antarctic Research Expeditions Scientific Reports, Series A* (IV) *Glaciology*, Publ. No. 108.

Clifford, P. M. 1972. Behaviour of an Archean granitic batholith. *Can. J. Earth Sci.* **9**, 71–77.

Cobbold, P. R. & Quinquis, H. 1980. Development of sheath folds in shear regimes. *J. Struct. Geol.* **2**, 119–126.

Coward, M. P. & Potts, G. 1983. Complex strain pattern development at the frontal and lateral tips to shear zones and thrust zones. *J. Struct. Geol.* **5**, 383–399.

Duncan, I. J. 1982. Strain in polyphase deformed fold belts: the case against constrictional incremental strains, stretching lineations and shear folding. *Geol. Soc. Am.* (Abst. with Programs) **14**, 479.

Elliott, D. 1972. Deformation paths in structural geology. *Bull. geol. Soc. Am.* **83**, 2621–2638.

Fry, N. 1979. Random point distributions and strain measurements in rocks. *Tectonophysics* **60**, 89–106.

Goldstein, A. G. 1980. Magnetic susceptibility anisotropy of mylonites from the Lake Char mylonite zone, southeastern New England. *Tectonophysics* **66**, 197–211.

Hambrey, M. J. 1975. The origin of foliation: evidence from some Norwegian examples. *J. Glaciol.* **14**, 181–185.

Hambrey, M. J. 1977. Foliation, minor folds and strain in ice. *Tectonophysics* **39**, 397–416.

Hambrey, M. J. & Milnes, A. G. 1977. Structural geology of an Alpine glacier (Griegsgletscher, Valais, Switzerland). *Eclog. geol. Helv.* **70**, 667–684.

Hambrey, M. J. & Müller, F. 1978. Structures and ice deformation in the White Glacier, Axel Heiberg Island, Northwest Territories, Canada. *J. Glaciol.* **20**, 41–66.

Hooke, R. LeB. & Hudleston, P. J. 1978. Origin of foliation in glaciers. *J. Glaciol.* **20**, 285–299.

Hossack, J. R. 1968. Pebble deformation and thrusting in the Bygdin area (southern Norway). *Tectonophysics* **5**, 315–339.

Hudleston, P. J. 1976a. Recumbent folding in the base of the Barnes Ice Cap, Baffin Island, Northwest Territories, Canada. *Bull. geol. Soc. Am.* **87**, 1684–1692.

Hudleston, P. J. 1976b. Early deformational history of Archean rocks in the Vermilion district, northeastern Minnesota. *Can. J. Earth Sci.* **13**, 579–592.

Hudleston, P. J. 1977a. Similar folds, recumbent folds and gravity tectonics in ice and rocks. *J. Geol.* **85**, 113–122.

Hudleston, P. J. 1977b. Progressive deformation and development of fabric across zones of shear in glacial ice. In: *Energetics of Geological Processes* (edited by Saxena, S. & Bhattacharji, S.). Springer, New York, 121–150.

Hudleston, P. J. & Hooke, R.LeB. 1980. Cumulative deformation in the Barnes Ice Cap and implications for the development of foliation. *Tectonophysics* **66**, 127–146.

Minnigh, L. D. 1979. Structural analysis of sheath folds in a meta-chert from the Western Italian Alps. *J. Struct. Geol.* **1**, 275–282.

Ragan, D. M. 1969. Structures at the base of an ice fall. *J. Geol.* **77**, 647–667.

Ramsay, J. G. 1980. Shear zone geometry: a review. *J. Struct. Geol.* **2**, 83–99.

Ramsay, J. G. 1981. Tectonics of the Helvetic nappes. In: *Thrust and Nappe Tectonics* (edited by McClay, K. R. & Price, N. J.). *Spec. Publs geol. Soc. Lond.* **9**, 151–158.

Talbot, C. J. 1979. Fold trains in a glacier of salt in southern Iran. *J. Struct. Geol.* **1**, 5–18.

Wegmann, C. E. 1963. Tectonic patterns at different levels. *Trans. Proc. geol. Soc. S. Afr* **66**, 1–78.